[논 문] 한국재료학회지
Korean J. Mater. Res.
Vol. 33, No. 3 (2023)

https://doi.org/10.3740/MRSK.2023.33.3.95

Effect of Al on Structural and Magnetic Characteristics of $CoCrFeNiMnAl_x$ High Entropy Alloys

Majid Tavoosi†, Ali Ghasemi, Gholam Reza Gordani, and Mohammad Reza Loghman Estarki†

Department of Materials Engineering, Malek Ashtar University of Technology, Isfahan 83157-13115, Iran

(Received January 25, 2023 : Revised February 17, 2023 : Accepted February 19, 2023)

Abstract This research examines the effect of adding aluminum on the structural, phasic, and magnetic properties of CoCrFeNiMnAl_x high-entropy alloys. To this aim, the arc-melt process was used under an argon atmosphere for preparing cast samples. The phasic, structural, and magnetic properties of the samples were characterized by x-ray diffraction (XRD), scanning electron microscopy (SEM), and vibrational magnetometry (VSM) analyses. Based on the results, the addition of aluminum to the compound caused changes in the crystalline structure, from FCC solid solution in the CoCrFeNiMn sample to CoCrFeNiMnAl BBC solid solution. It was associated with changes in the magnetic property of $CoCrFeNiMnAl_x$ high-entropy alloys, from paramagnetic to ferromagnetic. The maximum saturation magnetization for the CoCrFeNiMnAl casting sample was estimated to be around 79 emu/g. Despite the phase stability of the FCC solid solution with temperature, the solid solution phase formed in the CrCrFeNiMnAl high-entropy compound was not stable, and changed into FCC solid solution with temperature elevation, causing a reduction in saturation magnetization to about 7 emu/g.

Key words high-entropy alloys, magnetic properties, mechanical alloying, casting, solid solution.

1. Introduction

High-entropy alloys contain five or more alloy elements, such that the percentage of each alloy is the same or very close to each other. These alloys can be introduced as the newest group of alloys, introduced to the scientific community in 2005, and attracted a great deal of attention because of their special features.[1-5] From among different types of high-entropy alloys, CoCrFeNi alloys have attracted much attention due to their attractive magnetic behavior, with many scientists attempting to precisely characterize and evaluate the structural and magnetic properties of this compositional group. Preliminary investigations about this compositional group have shown that the crystalline structure of solid solution forms, following which the final magnetic properties heavily depend on the type of added elements, and the effect of different elements should be evaluated on these properties.

For example, Wang et al.[6] examined the effect of titanium elements on the magnetic and mechanical properties of the $FeCoCrCuNiTi_x$ alloy system. They showed that different percentages of this element can change the final crystalline structure from FCC solid solution to a structure composed of initial FCC solid solution, BCC eutectic phase mixture, Fe_2Ti intermetallic phase as well as some amorphous phase. This caused a change in magnetic behavior from paramagnetic to superparamagnetic. Zhang et al.,[7] by investigating the effect of aluminum element on FeCoCrNiCuAl high-entropy alloy reported that this element can also change the final structure at different percentages from FCC solid solution to BCC. The maximum saturation magnetization obtained from this research was estimated at around 39 emu/g. In 2004, also Ma et al.[8] explored the effect of niobium on the microstructure and properties of $AlCoCrFeNb_xNi$ high-entropy alloys. They found that the niobium element had a considerable effect on

†Corresponding author
E-Mail : ma.tavoosi@gmail.com (M. Tavoosi, Malek Ashtar Univ. Technol.)
mrlestarki@mut-es.ac.ir (M. R. Loghman Estarki, Malek Ashtar Univ. Technol.)

reducing the saturation magnetization and final magnetic properties. Zaddach et al.[9] explored the magnetic properties of $Ni_{20}Fe_{20}Cr_{20}Co_{20}Zn_{15}Mn_5$ high-entropy alloy. They observed that in the presence of manganese and zinc in the composition, the coercivity increased up to 515 Oe and saturation magnetization up to 50 emu/g. Other research in this area includes those conducted by Xiaoxia Zhu et al.[10] on the FeSiBAlNiM (M = Co, Cu, Ag) compositional group, Li et al.[11] in the $FeCoNiAl_{0.25}Mn_{0.25}$ high-entropy compositional group, Wang et al.[12] on the magnetic and mechanical properties of FeSiBAlNi(Nb) high-entropy alloys, and Yu et al.[13] about CoCrFeCuNi and CoCrFeMnNi high-entropy alloys.

Despite extensive research performed about this compound, the effect of the presence of aluminum on the structural and magnetic properties of this compound has not been evaluated precisely and needs further careful investigation. In addition, the structural and magnetic changes of this compound with temperature have not been assessed precisely, which again warrants investigation. Based on the mentioned points, this research aimed to investigate the structural, thermal, and magnetic properties of the $CoCrFeNiMnAl_x$ compositional group in the presence of different percentages of aluminum.

2. Experimental Procedure

In this research, primary elements of cobalt, iron, manganese, chromium, nickel, and aluminum with purity above 99 % were used for synthesizing three compounds of $CoCrFeNiMnAl_x$ high-entropy alloys, according to Table 1. To prepare casting ingots for alloy samples, the arc-melt process was used in an argon atmosphere. For melt homogeneity, this process was replicated three times for each compound. The heat treatment of the samples was done within the range of 700~1,000 °C for 2 h under an argon gas atmosphere.

For phase studies of the prepared samples, XRD test was used via PW3710 (Phillips Co.) device under voltage 40 kV and current 0.05 Amperes. In this method, CuK_α single ray was used with the wavelength 1.5404 Å and nickel filter, with the diffraction angle (2θ) chosen within 20~90°. The results obtained from this test were analyzed by Xpert High-score software and with a comparison against the standard card. Structural investigations of the obtained samples were followed via a scanning electron microscopy (SEM) device (VEGA-TESCAN-XMU). The magnetic properties of the researched samples (saturation magnetization and coercivity) were evaluated using a vibrational sample magnetometer (VSM).

3. Results and Discussion

According to references, the formation of the simple solid solution phase in a multicomponent alloy system depends on the extent of mixture enthalpy changes (ΔH_{mix}), mixture entropy changes (ΔS_{mix}), and atomic size difference parameter (δ) of the constituent elements. In this regard, the conditions of formation of a simple solid solution include $-23 \leq \Delta H_{mix} \leq 7$ kJ/mol, $\delta \leq 8.5$ %, and $11 \leq \Delta S_{mix} \leq 19.5$ J/K · mol.[1-3] The theoretical calculations done about all the examined compounds show that the value of δ for all compounds ranges within 5~6, the ΔH_{mix} value within -10~12 kJ/mol, and ΔS_{mix} larger than 11 kJ/mol. This means that theoretically, there is the possibility of the formation of a solid solution in all three compounds. In this regard, XRD patterns related to the three different compounds presented in Table 1 are displayed in Fig. 1. As seen, changes in the chemical composition and the addition of an aluminum element to the compound have had

Table 1. Chemical composition of the examined samples through the casting process in this research.

Sample No.	Amount (atomic percentage)					
	Co	Fe	Mn	Cr	Ni	Al
1	20	20	20	20	20	-
2	18.4	18.4	18.4	18.4	18.4	8
3	16.66	16.66	16.66	16.66	16.66	16.66

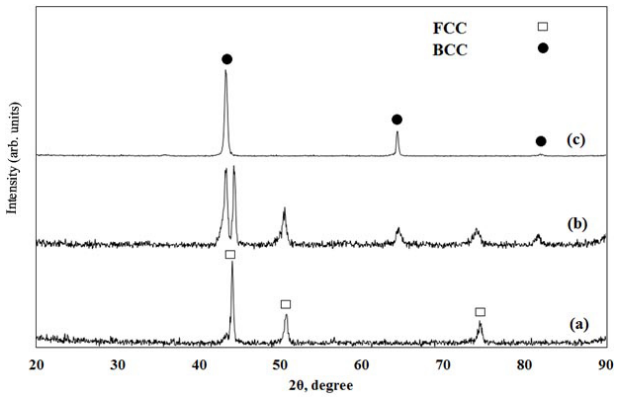

Fig. 1. The XRD patterns of $CoCrFeNiMnAl_x$ high entropy alloys, (a) x = 0, (b) x = 8 and (c) x = 16.

considerable effects on the phase structure of the examined compound. It is seen that the XRD pattern related to the CoCrFeNiMn alloy compound, which lacks aluminum, only contains the peaks related to FCC solid solution. There is no sign of the formation of unwanted intermetallic compounds or BCC solid solution in it. This can be demonstrated based on SEM images of the mentioned compound in Fig. 2.

According to Fig. 1, with the addition of 8 atomic percent aluminum element to the compound, alongside the peaks related to the FCC solid solution phase, the solid solution phase peaks with BCC structure have also been formed. This means that the presence of aluminum has been able to enhance the stability of the BCC solid solution phase, which is a magnetic phase. The XRD pattern related to the sample containing 16 atomic percent of aluminum in Fig. 1, reveals that in comparison to previous samples, for this sample the FCC solid solution phase peaks have been eliminated, and only the BCC solid solution phase peaks are present within the structure. According to references, stabilization of the FCC solid solution phase in this compound can be justified considering the valence electron concentration (VEC). This means that the FCC phase forms at VEC values larger than 8, and the BCC phase at VEC values smaller than 6.87. The VEC value for the FCC stabilizers such as Co and Ni is 9 and 10, while BCC stabilizers such as Al have a VEC of 3. This suggests that the addition of aluminum elements leads to a reduction of VEC and an increased tendency to form of BCC phase.[2)]

For examining the effect of the presence of aluminum on the magnetic properties of CoCrFeNiMnAl$_x$ high-entropy alloys, the magnetic hysteresis loops of the discussed samples are shown in Fig. 3. As seen, the magnetic properties of the high-entropy alloys are heavily dependent on the aluminum element percentage, and with an increase in the percentage of this element in the composition, it changes from paramagnetic to ferromagnetic. Alteration of the magnetic behavior of the mentioned compound upon adding aluminum element can be attributed to BCC solid solution phase formation within the structure as well as stabilization of this phase. In this regard, the maximum saturation magnetization value is attributed to the sample containing 16 atomic percent aluminum with about 79 emu/g.

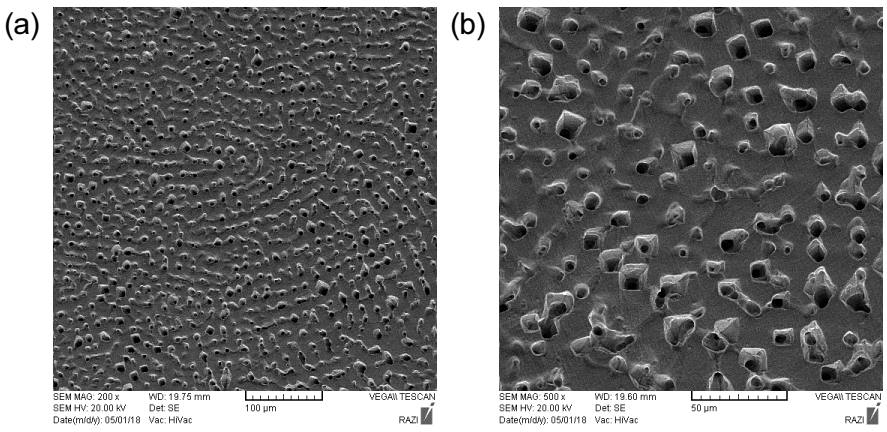

Fig. 2. The SEM micrographs of CoCrFeNiMn high entropy alloy in two magnifications.

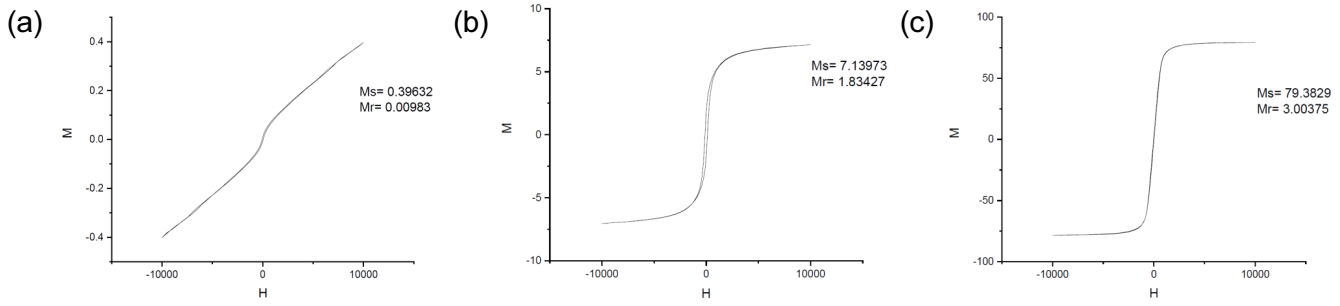

Fig. 3. The VSM hysteresis loops of CoCrFeNiMnAl$_x$ high entropy alloys, (a) x = 0, (b) x = 8, and (c) x = 16.

After the development of the FCC single-phase solid solution structure in the compound without aluminum plus the BCC single-phase solid solution in the sample containing 16 atomic percent aluminum, next it was attempted to explore the thermal stability of the resulting solid solution phases. In this regard, at 700, 850, and 1,000 °C, the samples were annealed for 1 h and then quenched in water. The XRD patterns related to the CoCrFeNiMn high-entropy alloy after the annealing are observed in Fig. 4. The notable point in this figure is the phase stability of the FCC solid solution, meaning that with an elevation of temperature regarding the CoCrFeNiMn high-entropy compound, this compound has been able to preserve its crystalline structure up to high temperatures. The lack of formation of intermetallic compounds, regular solid solution phases, as well as BCC solid solution structure in this regard, are notable. This can be proven based on SEM images of the examined compound in Fig. 5. As observed, the samples annealed at different temperatures have similar structures; the only notable difference regarding these samples is related to the size of the resulting phase, which has grown with temperature. Considering the stability of the FCC nonmagnetic solid solution phase in this sample with temperature, it is expected that the samples annealed at higher temperatures would still be nonmagnetic and annealing operations

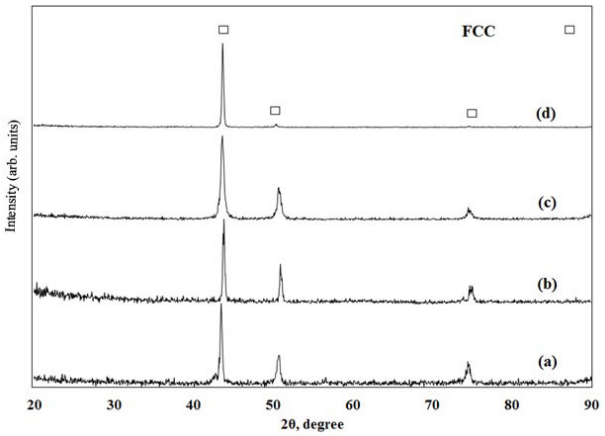

Fig. 4. The XRD patterns of CoCrFeNiMn high entropy alloy, (a) before and after annealing at (b) 700 °C, (c) 850 °C and (d) 1,000 °C for 1 h and quenching in cold water.

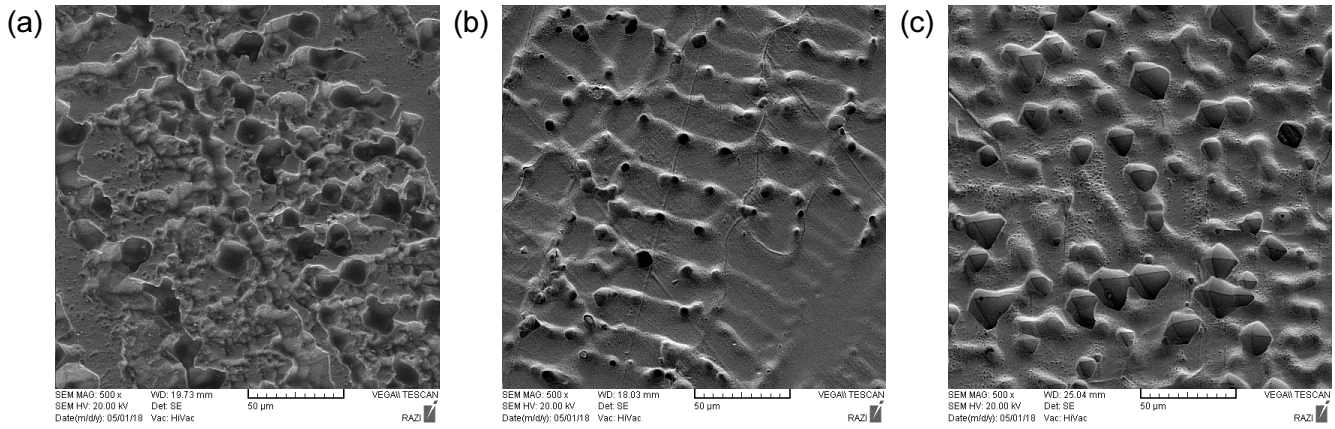

Fig. 5. The SEM micrographs of CoCrFeNiMn high entropy alloy, after annealing at (a) 700 °C, (b) 850 °C and (c) 1,000 °C for 1 h and quenching in cold water.

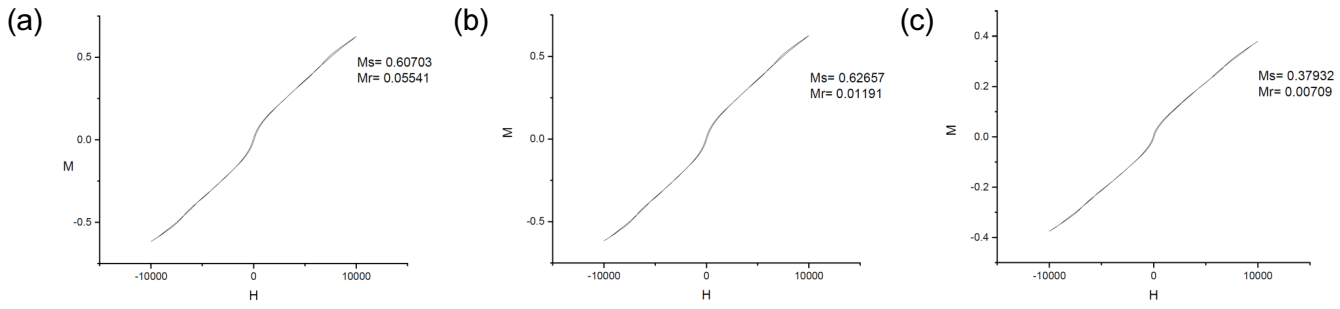

Fig. 6. The VSM hysteresis loops of CoCrFeNiMn high entropy alloy, after annealing at (a) 700 °C, (b) 850 °C and (c) 1,000 °C for 1 h and quenching in cold water.

would have no effect on their magnetic properties. This claim can be proven based on the relevant hysteresis curves in Fig. 6. As observed, the samples annealed at different temperatures, as with the sample obtained from casting, are nonmagnetic, confirming the solid solution phase stability in this alloy with temperature.

A literature review[6-16] suggests that the CoCrFeNiMnAl$_x$ high-entropy compositional group shows better magnetic behavior compared to other similar groups.

Similar to the previous sample, Fig. 7 depicts the XRD patterns related to the CoCrFeNiMnAl high-entropy compound with the crystalline structure of BCC solid solution after annealing process at different temperatures as well as quenching in water. As seen, considerable changes have occurred with temperature elevation in this sample. Unlike the previous sample, the BCC solid solution phase for the CoCrFeNiMnAl high-entropy alloy has not been stable, and with the increase in temperature, it gradually transforms into FCC solid solution phase. The BCC to FCC solid solution phase conversion in this case is very similar to the allotropic phase transformation of pure iron with temperature elevation. This type of phase transformation is assigned to network vibrations and thermal entropy with temperature enhancement, causing the BCC solid solution structure to destabilize, while the FCC solid solution phase forms.[17-30] In this regard, the magnetic hysteresis loops of the examined sample after the annealing process at different temperatures are presented in Fig. 8. Expectedly, the BCC to FCC phase transformation has had a considerable impact on the magnetic properties of the samples, and with temperature elevation, the extent of saturation magnetization has dropped from about 79 emu/g for the cast sample to around 7 emu/g for the sample annealed at 1,000 °C.

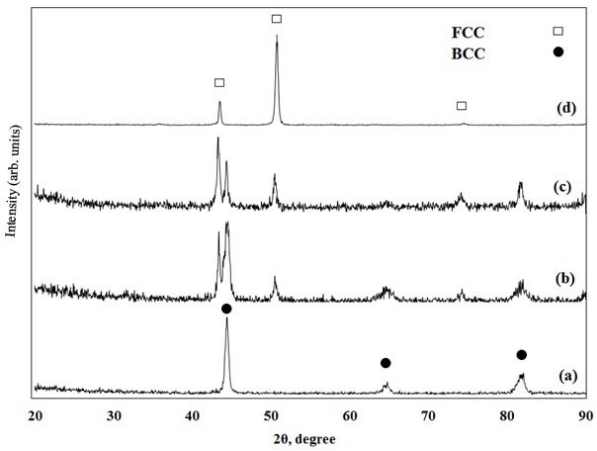

Fig. 7. The XRD patterns of CoCrFeNiMnAl high entropy alloy, (a) before and after annealing at (b) 700 °C, (c) 850 °C and (d) 1,000 °C for 1 h and quenching in cold water.

4. Conclusion

This research explored the effect of the presence of aluminum on the structural, phasic, and magnetic properties of CoCrFeNiMnAl$_x$ high-entropy alloys. The results revealed that the aluminum element has a considerable impact on the structure and properties of the mentioned high-entropy compound. The addition of aluminum caused a change in the crystalline structure from FCC solid solution in the CoCrFeNiMn sample to the BCC solid solution in the CoCrFeNiMnAl. The phase transformation of the FCC solid solution to BCC upon adding aluminum to the compound led to changes in the magnetic behavior of the CoCrFeNiMnAl$_x$ from paramagnetic to ferromagnetic. The maximum saturation magnetization for the cast sample CoCrFeNiMnAl was estimated at around 79 emu/g. Despite FCC solid solution phase stability with temperature, the solid solution phase formed in the CoCrFeNi

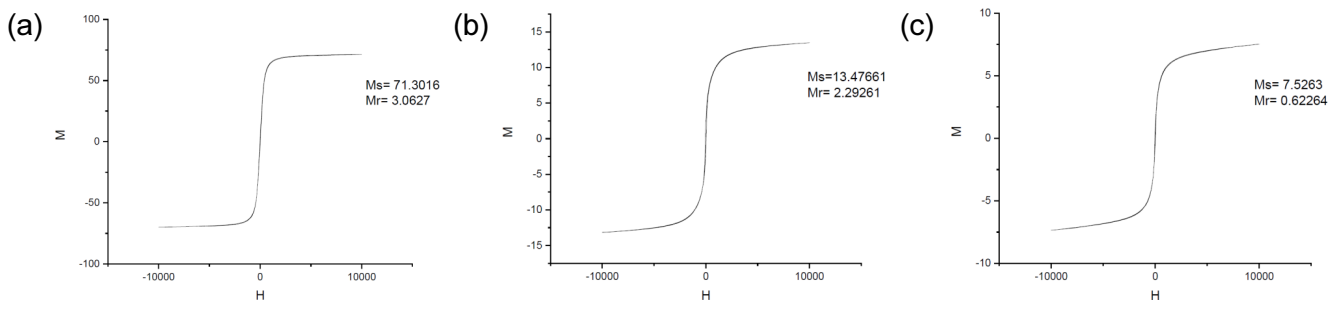

Fig. 8. The VSM hysteresis loops of CoCrFeNiMnAl high entropy alloy, after annealing at (a) 700 °C, (b) 850 °C and (c) 1,000 °C for 1 h and quenching in cold water.

MnAl high-entropy compound was not high, and with the rise of temperature, it would change to FCC solid solution. This transformation heavily affects the final magnetic properties and is associated with a reduction of saturation magnetization to about 7 emu/g.

References

1. B. S. Murty, J. W. Yeh and S. Ranganathan, High-entropy alloys, Butterworth-Heinemann (2014).
2. M. C. Gao, J. W. Yeh, P. K. Liaw and Y. Zhang, High-entropy alloys fundamentals and applications, Springer (2016).
3. Y. Zhang, T. T. Zuo, Z. Tang, M. C. Gao, K. A. Dahmen, P. K. Liaw and Z. P. Lu, Prog. Mater. Sci., **61**, 1 (2014).
4. X. Yang and Y. Zhang, Mater. Chem. Phys., **132**, 233 (2012).
5. Y. F. Kao, S. K. Chen, T. J. Chen, P. C. Chu, J. W. Yeh and S. J. Lin, J. Alloys Compd., **509**, 1607 (2011).
6. X. Wang, Y. Zhang, Y. Qiao and G. Chen, Intermetallics, **15**, 357 (2007).
7. K. B. Zhang, Z. Y. Fu, J. Y. Zhang, J. Shi, W. M. Wang, H. Wang, Y. C. Wang and Q. J. Zhang, J. Alloys Compd., **502**, 295 (2010).
8. S. G. Ma and Y. Zhang, Mater. Sci. Eng., A, **532**, 480 (2012).
9. A. J. Zaddach, C. Niu, A. A. Oni, M. Fan, J. M. LeBeau, D. L. Irving and C. C. Koch, Intermetallics, **68**, 107 (2016).
10. X. Zhu, X. Zhou, S. Yu, C. Wei, J. Xu and Y. Wang, J. Magn. Magn. Mater., **430**, 59 (2017).
11. P. Li, A. Wang and C. Liu, J. Alloys Compd., **694**, 55 (2017).
12. J. Wang, Z. Zheng, J. Xu and Y. Wang, J. Magn. Magn. Mater., **355**, 58 (2014).
13. P. Yu, L. Zhang, H. Cheng, H. Zhang, M. Ma, Y. Li, G. Li, P. Liaw and R. Liu, Intermetallics, **70**, 82 (2016).
14. C. Z. Yao, P. Zhang, M. Liu, G. R. Li, J. Q. Ye, P. Liu and Y.-X. Tong, Electrochim. Acta, **53**, 8359 (2008).
15. T. Qi, Y. Li, A. Takeuchi, G. Xie, H. Miao and W. Zhang, Intermetallics, **66**, 8 (2015).
16. M. Lucas, D. Belyea, C. Bauer, N. Bryant, E. Michel, Z. Turgut, S. Leontsev, J. Horwath, S. Semiatin and M. McHenry, J. Appl. Phys., **113**, 17A923 (2013).
17. J. Müssig and N. Graupner, Prog. Adhes. Adhes., **6**, 69 (2021).
18. P. Brown and P. Mazumder, Prog. Adhes. Adhes., **6**, 709 (2021).
19. C. Della Volpe and S. Siboni, Rev. Adhes. Adhes., **10**, 47 (2022).
20. A. Mojtahedi, H. Hokmabady, M. Kouhi and S. Mohammadyzadeh, Compos. Struct., **279**, 114794 (2022).
21. M. Ghasemvand, B. Behjat and S. Ebrahimi, J. Adhes., **98**, 1 (2022).
22. S. D. Wani and A. S. Mundada, Int. J. Pharm. Res. Technol., **11**, 1 (2021).
23. A. K. Netam, V. P. Bhargava, R. Singh and P. Sharma, J. Complementary Med. Res., **12**, 204 (2021).
24. N. K. A. Dwijendra, I. Patra, Y. M. Ahmed, Y. M. Hasan, Z. M. Najm, Z. I. A. Mashhadani and A. Kumar, Monatsh. Chem., **153**, 873 (2022).
25. S. Chupradit, A. T. Jalil, Y. Enina, D. A. Neganov, M. S. Alhassan, S. Aravindhan and A. Davarpanah, J. Nanomater., **2021**, 1 (2021).
26. K. Hachem, S. A. Jasim, M. E. Al-Gazally, Y. Riadi, G. Yasin, A. T. Jalil, M. M. Abdulkadhm, M. M. Saleh, M. N. Fenjan, Y. F. Mustafa and A. D. Khalaji, J. Chin. Chem. Soc., **69**, 512 (2022).
27. X. Hu, A. H. Derakhshanfard, I. Khalid, A. T. Jalil, M. J. C. Opulencia, R. B. Dehkordi, D. Toghraie, M. Hekmatifar and R. Sabetvand, J. Taiwan Inst. Chem. Eng., **135**, 104396 (2022).
28. R. O. Saleh, D. O. Bokov, M. N. Fenjan, W. K. Abdelbasset, U. S. Altimari, A. T. Jalil, L. Thangavelu, W. Suksatan and Y. Cao, J. Mol. Liq., **352**, 118676 (2022).
29. S. Chupradit, M. KM Nasution, H. S. Rahman, W. Suksatan, A. T. Jalil, W. K. Abdelbasset, D. Bokov, A. Markov, I. N. Fardeeva, G. Widjaja, M. N. Shalaby, M. M. Saleh, Y. F. Mustafa, A. Surendar and R. Bidares, Anal. Biochem., **654**, 114736 (2022).
30. I. Raya, S. Chupradit, M. M. Kadhim, M. Z. Mahmoud, A. T. Jalil, A. Surendar, S. T. Ghafel, Y. F Mustafa and A. N. Bochvar, Chin. Phys. B, **31**, 016401 (2021).

Author Information

Majid Tavoosi

Associate Professor, Department of Materials Engineering, Malek Ashtar University of Technology

Ali Ghasemi

Professor, Department of Materials Engineering, Malek Ashtar University of Technology

Gholam Reza Gordani

Associate Professor, Department of Materials Engineering, Malek Ashtar University of Technology

Mohammad Reza Loghman Estarki

Associate Professor, Department of Materials Engineering, Malek Ashtar University of Technology